

Initiation of bacteriophage ϕ 29 DNA packaging and effect of the gp3 terminal protein studied by an optical tweezers assay

John Peter Rickgauer^{*}, Derek N. Fuller^{*}, Shelley Grimes[†], Paul J. Jardine[†],
Dwight L. Anderson^{†#}, Douglas E. Smith^{*}

^{}Department of Physics, University of California, San Diego
Mail Code 0379, 9500 Gilman Drive, La Jolla, CA 92093*

*[†]Department of Diagnostic and Biological Sciences, and [#]Department of Microbiology, University of
Minnesota, 18-246 Moos Tower, 515 Delaware Street SE, Minneapolis, MN 55455*

A key step in the assembly of many viruses is the packaging of DNA into a precursor capsid (prohead) by the action of an ATP-powered molecular motor. Here we describe a new optical tweezers assay that permits study of the initiation of DNA packaging into single bacteriophage ϕ 29 proheads. We demonstrate an assembly sequence whereby prohead-ATPase complexes are assembled *in vitro* and then bind a target DNA molecule within a few seconds and began translocation within one second. This measurement was facilitated by a microfluidic system that permits rapid loading of two microspheres into two optical traps. We found that the DNA terminal protein gp3 had a dramatic effect on the DNA-gp3 conformation during packaging initiation. The initial extended length of the DNA-gp3 tether varied from ~30-100% of the full-length substrate, showing that packaging did not generally involve binding of a free end of the DNA, and that DNA-gp3 had a higher-order structure. Digestion of gp3 with proteinase K eliminated this variability, resulting in uniform full-length tethers at initiation. These findings are consistent with previous electron microscopy studies showing that ϕ 29 DNA-gp3 forms lariats mediated by gp3 and suggest that DNA packaging initiates at the lariat loop junctions. In addition, sucrose gradient sedimentation studies showed that the gp16 motor protein could cleave the gp3-DNA, providing an explanation for the translocation of the short tethers in the optical tweezers assay. We found that this effect could also be avoided by simply using a DNA substrate lacking gp3. In particular, non-native DNAs generated by PCR, including *E. coli* and human sequences, were readily packaged with reproducible DNA terminal initiation, facilitating accurate measurement of the length of DNA packaged.

Running Title: Initiation of bacteriophage ϕ 29 DNA packaging

Introduction

A particularly striking step that occurs in the assembly of many double-stranded DNA viruses is the packaging of the viral genome into preformed precursor capsids (proheads) by a transiently assembled molecular motor complex^{1, 2, 3}. Although high-resolution structures of some dsDNA viruses and components of the packaging motor complexes have been determined^{4, 5, 6, 7}, the mechanism of DNA packaging, particularly the structural transitions involved in packaging initiation, is obscure. To elucidate the molecular dynamics of packaging, biophysical measurements are a complement to the structural, genetic and biochemical approaches.

The *Bacillus subtilis* bacteriophage $\phi 29$ is one of the simplest dsDNA phages and is an excellent model for investigating basic principles of viral assembly^{8, 9}. The 19.3 kilobase pair $\phi 29$ genome encodes twenty gene products. The DNA packaging motor is situated at a unique five-fold vertex in the 40nm by 50nm prohead. The motor consists of: the dodecameric head-tail connector comprised of gene product 10 (gp10), a ring of RNA molecules (prohead RNA, pRNA) attached to the narrow end of the connector, and multiple copies of the gp16 ATPase¹⁰. The structure of the connector has been determined by X-ray crystallography, and it has been proposed to play an important role in DNA translocation^{5, 11}.

The $\phi 29$ genome, like that of human adenovirus, has a terminal protein covalently bound to each 5' end (DNA-gp3). gp3 primes DNA replication¹², and the recent determination of this protein complexed with the $\phi 29$ DNA polymerase¹³ has yielded a model for the priming mechanism. gp3 also greatly enhances the efficiency and selectivity of DNA packaging in vitro¹⁴. Packaging initiation involves the interaction of the motor complex (connector/pRNA/ATPase) and the DNA-gp3 substrate, but little is known about the way this ensemble coordinates DNA binding and translocation.

Previously, we developed a method for studying single DNA molecule packaging using optical tweezers assay in which packaging activity was reconstituted in a completely defined system using purified components^{15, 16, 17}. We found that the DNA is packaged processively at speeds up to ~100 bp/s, and a high force of ~60 pN generated by the motor was needed to overcome high internal force resisting DNA confinement in the prohead. We assayed stalled complexes in which about one-third of the genome was already packaged in bulk, and therefore the dynamics of initiation of packaging and early translocation events could not be examined. Here, we present an improved

method in which DNA packaging is initiated in the optical tweezers, permitting study of the motor assembly sequence, time for binding of the DNA substrate, and initiation of translocation.

Results and Discussion

Assembly of DNA packaging complexes

In the standard *in vitro* packaging assay, the proheads, packaging ATPase gp16 and DNA-gp3 are mixed together in bulk¹⁰, and the order of interaction of the components is unclear. Here we controlled the sequence of the interactions leading to the initiation of packaging. Proheads and the packaging ATPase gp16 were assembled in the presence of the non-hydrolyzable ATP analog γ S-ATP, and these complexes were attached to antibody-coated microspheres. Restriction fragments of DNA-gp3 molecules were attached to streptavidin-coated microspheres via a biotin tag at the restriction site (see Materials and Methods).

Optical tweezers assay

Our measurement technique is illustrated schematically in Fig. 1. Two optical traps were formed in a thin fluid chamber filled with the packaging buffer containing ATP. A microsphere carrying tethered DNA was injected into the chamber via a small capillary tube and captured in one optical trap. A prohead-gp16-coated microsphere was injected via a second capillary tube and captured in the second trap. One optical trap was moved with respect to the other by means of a computer-controlled acousto-optic deflector (methods). Packaging was initiated by bringing these two microspheres into near contact for one second and then quickly separating them to probe for DNA binding. When a DNA molecule bound to the prohead-motor complex, it formed a tether between the two microspheres that was stretched taut when the traps were separated. The binding was detected by measuring the tensioning force acting on the microspheres. A DNA binding event was usually detected after only a few approach cycles, as shown in Fig. 1.

The prohead-motor complex bound DNA very rapidly—within a few seconds after the DNA was brought into close proximity. When a binding event was detected, the DNA was stretched until the tension reached 5-10 pN, and the separation between the two optical traps was then fixed. Translocation of the DNA by the motor was detected as a subsequent rise in the measured tension due to the progressive shortening of the DNA tether, as shown in Fig. 1. In most cases, binding events were followed by active DNA translocation, generally detected within one second of binding.

After the initiation of translocation, the tension in the DNA was allowed to build until breakage of the tether occurred. Breakage is likely due to disruption of the antibody-prohead linkage, since the biotin-streptavidin linkage of the DNA is much stronger, or to stripping of the motor. In these experiments, the concentration of the DNA was lowered to the point where only single DNA binding events were usually observed, as distinguished by the known characteristic elastic response of single DNA molecules¹⁸. Breakage of the tether usually occurred in a single step, providing further confirmation that we were recording the packaging of a single DNA molecule.

Stability of the active complex

Notably, incubation with γ S-ATP was essential for the formation of active prohead-gp16 motor complexes. If it was omitted, or if only ATP was used, tether formation was not observed. In addition, after the microspheres carrying the prohead-gp16 complexes were injected into the fluid chamber, we found that it was essential to bring the bead carrying the DNA in quickly to observe packaging. This may be due to disruption or inactivation of the prohead-gp16 complex as γ S-ATP was exchanged with ATP in the chamber. Implementation of a dual optical tweezers system allowed us to quickly load the microspheres into the traps and to probe for DNA binding and translocation within 5-10 seconds. When prohead-gp16 complexes were exposed to ATP for longer than two minutes prior to DNA contact, the success of initiation of packaging decreased by ~90% (N=75 trials). Thus, γ S-ATP appears to stabilize an active form of the prohead-gp16 complex in the absence of DNA, whereas ATP destabilizes it. Once the motor engaged the DNA, the active complex was stable in the presence of ATP and remained engaged in highly processive translocation. In this sense, engaged DNA is an essential component of the active motor complex.

Variable conformations of DNA-gp3 at initiation

In the initiation measurements, we found that the initial extended lengths of the translocating DNA-gp3 tethers were highly variable, ranging from 30 to 100% of the full-length of the DNA substrate (Fig. 2A&B). Such variability was not revealed in our earlier studies using partly packaged complexes, where variability could be attributed to lack of synchronization of different complexes in the bulk reaction and the variable time lapse required to tether the DNA¹⁵. Here, however, we found that the tether length variability at the start of packaging was inherent, showing that the DNA-gp3 has a complex structure and does not generally bind to the motor by a free end.

Role of the DNA terminal protein

Electron microscopy studies found that ϕ 29 DNA-gp3 forms gp3-mediated loops and that gp16 tends to bind to the loop junctions¹⁹. The presence of such loops could reconcile the variable tether lengths observed in the optical tweezers if packaging initiates with binding of the prohead-gp16 complex to the DNA-gp3 loop junction. We found that the variability is directly attributable to gp3, since it disappeared when the DNA-gp3 was proteolysed by treatment with proteinase K (Fig. 2C&D). Both the left end (15 kb) and right end (4 kb) restriction fragments with proteolysed gp3 were readily packaged with full tether lengths at initiation. Further, non-native DNA molecules generated by PCR were packaged with full-length tethers at initiation, showing that packaging was not sequence dependent: bacteriophage λ , *E. coli* and human DNA sequences were readily packaged (data not shown). The observed single-molecule packaging of non-gp3 DNA, which is packaged inefficiently in bulk *in vitro* packaging assays¹⁴, appears to have been facilitated by forcing the DNA and proheads into close proximity via mechanical manipulation.

As seen in Fig. 2C&D, when testing non-gp3 DNA we observed left end (15 kbp) and right end (4 kbp) tethers, and the 4 kb tethers were more frequent, indicating that the shorter non-gp3 molecule binds more efficiently in our assay. In initial measurements with gp3-DNA we observed tethers ranging in length from ~1 to 15 kb (data not shown), suggesting that both the 4 kb and 15 kb DNAs can form loops. We recorded the data in Fig. 2A&B in such a manner as to isolate the behavior of the 15 kb molecule. Since tethers <4 kbp could be due to looping of either the 4 kb or 15 kb molecule we used an automatic control program to stretch slightly past 4 kbp (breaking any shorter tethers) before triggering a tether length measurement. Thus, these measurements report on the possible lengths >4 kb of the 15 kbp DNA only. We clearly find that gp3-DNA exhibits short initial tether lengths between 4 kb and 15 kb, whereas non-gp3 DNA does not.

DNA translocation

To further investigate the effect of gp3 on packaging, additional measurements were made with a 34.4 kbp ϕ 29 gp3-DNA-lambda DNA hybrid construct that was ~80% longer than the wild-type ϕ 29 genome. Use of this construct allowed us to detect both the initiation and completion of packaging (Fig. 3). We found that, regardless of the initial tether length, a length of DNA approximately equal to the ϕ 29 genome length was packaged before DNA translocation stopped. This was also observed with non-gp3 DNA, except that the initial tether length was reproducible (Fig. 2). Thus, the tether length variability is not due to a rapid burst of packaging during the ~1 second

before the DNA was stretched to measure the tether length. We can also rule out that the motor disrupts and opens the loop because the tether only shortened and did not lengthen. If the prohead bound at the loop junction and disrupted the loop upon initiation of DNA translocation, a sudden increase in tether length to the full length of the template would be expected but this was not observed. We can also rule out packaging of the looped DNA (i.e., translocation of two or more widths of DNA simultaneously through the portal) because the same tether length is translocated independent of the starting length. If multiple widths of DNA were packaged in parallel, a smaller change in tether length would have been observed. This latter finding is consistent with structural studies showing that the portal channel is only large enough to accommodate a single width of dsDNA⁵.

A simple explanation for the packaging of shortened tethers is that the motor excises the looped section of DNA, and packages the remaining length of the substrate, as shown schematically in Fig. 4. Although DNA-gp3 alone is not cleaved in the reaction buffer^{14, 20, 21, 22}, sucrose gradient sedimentation analysis revealed that gp16 *can* induce cleavage of DNA-gp3 (Fig. 5). In repeated experiments such cleavage was only observed occasionally, but was very clearly observed in several independent experiments, and never observed with non-gp3 DNA or in the absence of gp16. We therefore conclude that gp16 does have the capability to cleave DNA-gp3, which provides a simple explanation for the packaging of short tethers in the optical tweezers assay.

Cleavage must not generally occur during packaging *in vivo* (in the infected *B. subtilis* host) since the complete genome is generally packaged into mature viruses. Our interpretation of the intermittent cleavage observed *in vitro* is that it may be consequence of the reported gp16-induced supercoiling of the DNA-gp3¹⁹. This supercoiling has been proposed to occur by a gyrase-like mechanism in which one segment is transiently cleaved, another segment is “passed through”, and the cut is resealed. The supercoiling has been shown to facilitate binding of gp16-DNA-gp3 complexes to the connector ring (gp10) on the prohead²³, which is an alternate sequence by which DNA packaging can initiate¹⁹. We propose that irreversible cleavage may occasionally occur during such gyrase-like action, and that it occurs more frequently in the optical tweezers assay due to the tension applied across the DNA. We note that tension-induced enhancement of DNA cleavage was observed in our previous optical tweezers studies of the HindIII endonuclease²⁴.

Conclusions

We showed that gp16 can preassemble on the prohead and then rapidly bind and begin packaging of a target DNA molecule. We presented evidence that the gp3 mediated DNA loops observed in previous electron microscope studies are present during initiation of active DNA packaging in ϕ 29. We also showed that such looping can be avoided by using non-gp3 DNA, which allows the packaging of the whole ϕ 29 genome length to be accurately measured in the optical tweezers assay. Finally, we showed that non-native DNA constructs produced by PCR could be readily packaged. The methods described here will have many applications in future studies. The ability to reproducibly initiate packaging in real time paves the way for more precise and detailed studies of the function of the ϕ 29 motor, including characterization of the nature of the DNA-motor interactions and the energetics governing DNA confinement in the prohead. Moreover, the approach presented here for initiating packaging is applicable to the study of DNA packaging in other viruses, such as bacteriophages λ and T4^{2, 25}.

Methods

Sample preparation

Bacteriophage ϕ 29 proheads, DNA-gp3, and gp16 were purified as described previously¹⁹. *Spe*I DNA-gp3 fragments (a 14.9 kbp left end and a 4.4 kb right end) and the λ - ϕ 29 DNA-gp3 hybrid construct was prepared and labeled as described previously¹⁵. Digested DNA-gp3 fragments were prepared by incubating 0.13 μ g/ μ l of DNA-gp3 with 0.3 μ g/ μ l proteinase K for 30 min at 65°C. The human and *E. coli* DNA constructs were prepared by PCR as described previously²⁶. Prohead-motor complexes were assembled as follows: 2 μ g of proheads containing 120-base pRNA were mixed with 0.25 μ g of gp16 in 10 μ l of 0.5x TMS buffer (50 mM Tris-HCl buffer (pH 7.8), 50 mM NaCl, 5 mM MgCl₂) for 2 min; γ S-ATP (Roche Applied Science) was then added to a final concentration of 0.4 mM, and the sample was incubated for 45 min at room temperature.

Streptavidin-coated microspheres (2.2 μ m diameter, 5% w/v) and protein G-coated microspheres (2.1 μ m diameter, 5% w/v) were obtained from Spherotech and washed twice by centrifugation in phosphate buffered saline. The biotinylated DNA was tethered to the streptavidin microspheres as described previously²⁶. Anti-phage antibodies were bound to the protein G microspheres by incubating them for 10 min in a 1/10 dilution of rabbit antiserum prepared against ϕ 29, washing them five times in 0.5x TMS, and resuspending them in 1/10 volume of 0.5x TMS. 2 μ l of these microspheres were added to 4.5 μ l of the prohead-motor complexes and 10 μ l of 0.5x

TMS and incubated for 45 min. Packaging measurements were carried out in 0.5x TMS supplemented with 0.5 mM ATP.

Optical tweezers

A dual optical tweezers system similar to that used in studies of actin-myosin interactions was used²⁷. In brief, a diode-pumped solid-state Nd:YAG laser (CrystaLaser) was split into two orthogonally polarized beams focused by a water-immersion microscope objective (Olympus, Plan Apochromat, 60x, 1.2 NA). One beam was steered by use of an acousto-optic deflector (Intraaction), and the second beam was fixed. The exiting beams were collected by a second, identical objective, and the deflections of the fixed beam were measured by imaging the back focal plane of this objective onto a position-sensing detector (On-Trak). The system was calibrated as describe previously²⁸.

During probing for DNA binding, the trap position was ramped back and forth at 10 $\mu\text{m/s}$. The force signal was recorded at 1 kHz, and the contour length of the DNA tether in basepairs was calculated from the measured end-to-end extension by use of the wormlike chain model, as described previously¹⁵.

Sample chamber and microsphere loading

The sample chamber was fabricated as a sandwich of two parallel 24 mm x 60 mm #1 microscope coverglasses (Fisher Scientific, Waltham, MA), separated by two $\sim 100 \mu\text{m}$ thick sheets of thermosetting epoxy film (#561-1-005, Ablefilm Laboratories, Rancho Dominguez, CA). Three parallel fluid channels were cut parallel to the long axis in the epoxy film using a sharp X-acto knife. The design of the chamber and flow system is illustrated schematically in Supplemental Fig. S2. Access holes ($\sim 1 \text{ mm}$ diam.) were drilled through one of the coverglasses using a CO_2 laser cutting system (Universal Laser Systems, Scottsdale, AZ). The holes were located at the ends of each of the three channels. The coverglasses and epoxyfilm were bonded together by heating at $120 \text{ }^\circ\text{C}$ for 2 hrs. The chamber was clamped onto a custom made metal holder, which also clamped the access holes to the flush ends of input/output tubes (PE-50 polyethylene tubing, Becton Dickinson, Franklin Lakes, NJ), which were held in place with epoxy and press-sealed against the flow chamber.

The optical traps were formed in the middle channel ($\sim 2.5 \text{ mm}$ width) and the two side channels ($\sim 1.5 \text{ mm}$ width) contained suspensions of the two different types of microspheres. The microspheres were injected from the side channels into the main channel via two capillary tubes (100 micron outer diameter, 30 micron inner diameter, type kg33 pyrex, Garner Glass Co., Claremont,

CA), which connected each side channel to the main channel. These capillaries were placed between the two sheets of epoxy film before the coverglasses were bonded together. The capillaries were carefully positioned so that their ends, from which the microspheres were delivered into the main chamber, were only a few hundred microns apart.

The microsphere solutions were flowed into the side channels by use of 1 ml tuberculin slip tip syringes (Becton Dickinson) connected to the input tubes (the syringe needle was coupled to the input tube by a short section of 1/32" tygon rubber tubing). The output tubes for the side channels were left as open standpipes. The flow of the microspheres from the side channels into the main channel was driven by gravity and thus controlled by adjusting the heights of the fluid levels of the output tubes. In this manner the flow could be adjusted so that the microspheres flowed out very slowly from the ends of the capillary tubes (one microsphere at a time, given the high dilution of microsphere solution). The packaging buffer was also introduced into the center channel by gravity-driven flow from an inverted 10 ml syringe with the plunger removed. A valve was incorporated (#86728, Hamilton Company, Reno, NV) so that we could turn the flow on or off.

The flow cell holder was attached to a micrometer-driven translation stage (Newport #461-XYZ, Newport Corp., Irvine, CA) so that it could be moved relative to the optical traps. The two microspheres were loaded into the traps as follows. We moved the stage to position the first trap next to the output of the first capillary tube and waited (typically a few seconds) until a microsphere came out and was trapped. We then moved the stage to position the second trap near the output of the second capillary tube and waited until a second microsphere was trapped. We then moved the stage to position the traps at least 200 μm away from the capillary outputs, to minimize the perturbation of hydrodynamic flows on the force measurements. The perturbation due to flow was <1 pN, which is small compared to the 5 pN and higher forces applied to stretch the DNA in our measurements.

References

1. Catalano, C. E. (2005). *Viral Genome Packaging Machines: An Overview*. Viral Genome Packaging Machines: Genetics, Structure, and Mechanism (Catalano, C. E., Ed.), Springer.
2. Kondabagil, K. R., Zhang, Z. & Rao, V. B. (2006). The DNA translocating ATPase of bacteriophage T4 packaging motor. *Journal of molecular biology* 363, 786-99.
3. Jardine, P. J. & Anderson, D. (2006). DNA packaging in double-stranded DNA bacteriophages. In *The Bacteriophages* (Calendar, R., ed.). Oxford Press.
4. Tao, Y., Olson, N. H., Xu, W., Anderson, D. L., Rossmann, M. G. & Baker, T. S. (1998). Assembly of a tailed bacterial virus and its genome release studied in three dimensions. *Cell* 95, 431-7.

5. Simpson, A. A., Tao, Y., Leiman, P. G., Badasso, M. O., He, Y., Jardine, P. J., Olson, N. H., Morais, M. C., Grimes, S., Anderson, D. L., Baker, T. S. & Rossmann, M. G. (2000). Structure of the bacteriophage phi29 DNA packaging motor. *Nature* 408, 745-50.
6. Fokine, A., Chipman, P. R., Leiman, P. G., Mesyanzhinov, V. V., Rao, V. B. & Rossmann, M. G. (2004). Molecular architecture of the prolate head of bacteriophage T4. *Proceedings of the National Academy of Sciences of the United States of America* 101, 6003-8.
7. Lander, G. C., Tang, L., Casjens, S. R., Gilcrease, E. B., Prevelige, P., Poliakov, A., Potter, C. S., Carragher, B. & Johnson, J. E. (2006). The structure of an infectious P22 virion shows the signal for headful DNA packaging. *Science* 312, 1791-5.
8. Anderson, D. & Reilly, B. (1993). Morphogenesis of Bacteriophage f29. In *Bacillus subtilis and other gram positive bacteria: Biochemistry, physiology, and molecular genetics* (Sonenshein, A., Hoch, J. A. & Losick, R., eds.), pp. 859-867. American Society for Microbiology, Washington D.C.
9. Anderson, D. & Grimes, S. (2005). The ϕ 29 DNA Packaging Motor: Seeking the Mechanism. In *Viral Genome Packaging Machines: Genetics, Structure, and Mechanism* (Catalano, C. E., ed.). Springer.
10. Grimes, S., Jardine, P. J. & Anderson, D. (2002). Bacteriophage phi 29 DNA packaging. *Adv Virus Res* 58, 255-94.
11. Guasch, A., Pous, J., Ibarra, B., Gomis-Ruth, F. X., Valpuesta, J. M., Sousa, N., Carrascosa, J. L. & Coll, M. (2002). Detailed architecture of a DNA translocating machine: the high-resolution structure of the bacteriophage phi29 connector particle. *J Mol Biol* 315, 663-76.
12. Salas, M. (1991). Protein-priming of DNA replication. *Annu Rev Biochem* 60, 39-71.
13. Kamtekar, S., Berman, A. J., Wang, J., Lazaro, J. M., de Vega, M., Blanco, L., Salas, M. & Steitz, T. A. (2006). The phi29 DNA polymerase:protein-primer structure suggests a model for the initiation to elongation transition. *The EMBO journal* 25, 1335-43.
14. Grimes, S. & Anderson, D. (1989). In vitro packaging of bacteriophage phi 29 DNA restriction fragments and the role of the terminal protein gp3. *J Mol Biol* 209, 91-100.
15. Smith, D. E., Tans, S. J., Smith, S. B., Grimes, S., Anderson, D. L. & Bustamante, C. (2001). The bacteriophage ϕ 29 portal motor can package DNA against a large internal force. *Nature* 413, 748-52.
16. Chemla, Y. R., Aathavan, K., Michaelis, J., Grimes, S., Jardine, P. J., Anderson, D. L. & Bustamante, C. (2005). Mechanism of force generation of a viral DNA packaging motor. *Cell* 122, 683-92.
17. Fuller, D., Rickgauer, J., Jardine, P., Grimes, S., Anderson, D. & Smith, D. (2007). Ionic effects on viral DNA packaging and portal motor function in bacteriophage phi29. *Proc Natl Acad Sci U S A* 104, 11245.
18. Smith, S. B., Cui, Y. & Bustamante, C. (1996). Overstretching B-DNA: the elastic response of individual double-stranded and single-stranded DNA molecules. *Science* 271, 795-9.
19. Grimes, S. & Anderson, D. (1997). The bacteriophage phi29 packaging proteins supercoil the DNA ends. *J Mol Biol* 266, 901-14.
20. Grimes, S. & Anderson, D. (1989). Cleaving the prohead RNA of bacteriophage phi 29 alters the in vitro packaging of restriction fragments of DNA-gp3. *J Mol Biol* 209, 101-8.
21. Grimes, S. & Anderson, D. (1990). RNA dependence of the bacteriophage phi 29 DNA packaging ATPase. *J Mol Biol* 215, 559-66.
22. Atz, R., Ma, S., Gao, J. L., Anderson, D. L. & Grimes, S. (2007). Alanine scanning and Fe-BABE probing of the bacteriophage phi29 prohead RNA-connector interaction. *J. Mol. Biol.* 369, 239.

23. Turnquist, S., Simon, M., Egelman, M. & Anderson, D. L. (1992). Supercoiled DNA wraps around the bacteriophage ϕ 29 head-tail connector. *Proc Nat Acad Sci USA* 89, 10479-10483.
24. Gemmen, G. J., Millin, R. & Smith, D. E. (2006). Tension-dependent DNA cleavage by restriction endonucleases: Two-site enzymes are “switched off” at low force. *Proc Nat Acad Sci USA* 103, 11555.
25. Feiss, M. & Catalano, C. E. (2005). *Bacteriophage Lambda Terminase and the Mechanism of Viral DNA Packaging*. *Viral Genome Packaging Machines: Genetics, Structure, and Mechanism* (Catalano, C. E., Ed.), Springer.
26. Fuller, D. N., Gemmen, G. J., Rickgauer, J. P., Dupont, A., Millin, R., Recouvreux, P. & Smith, D. E. (2006). A general method for manipulating DNA sequences from any organism with optical tweezers. *Nucleic Acids Res* 34, e15.
27. Simmons, R. M., Finer, J. T., Chu, S. & Spudich, J. A. (1996). Quantitative measurements of force and displacement using an optical trap. *Biophys J* 70, 1813-22.
28. Rickgauer, J. P., Fuller, D. N. & Smith, D. E. (2006). DNA as a metrology standard for length and force measurements with optical tweezers. *Biophys J* 91, 4253-4257.

Figure Legends

Fig. 1. Initiation measurement. **Left:** Schematic diagram showing the experimental configuration. Two microspheres are held in two optical traps. Pre-assembled prohead-gp16 complexes are bound to one microsphere (top, magnified view in red box). DNA molecules are tethered to a second microsphere (bottom, magnified view in green box). **Right:** Imposed trap separation (top graph) and measured force (bottom graph). To initiate DNA packaging the two microspheres were brought into near contact for ~1 second (decreasing trap separation to near zero) and then rapidly separated to probe for DNA binding. In this particular example no binding was detected in the first probing, but an event was detected after the second approach, as indicated by the sudden rise in force as the traps were separated (end of the blue section of the plot in the bottom graph). When the force rose to 5 pN, the trap separation was fixed (green section of the top and bottom graphs) and DNA translocation was detected as a progressive rise in force. The force rises due to the progressive tensioning of the DNA as the motor pulls it in.

Fig. 2. Initiation of DNA packaging with tethered ϕ 29 DNA-gp3 restriction fragments (a 14.9 kbp left end and 4.4 kbp right end). **(A)** Multiple measurements of force vs. trap separation showing initiation events. The trap separation was increased until the force rose to 5-10 pN whereupon the separation was fixed. The subsequent rise in force is due to the shortening of the tether due to DNA packaging. Only measurements on actively packaging complexes are shown. **(B)** Histogram of the initial DNA tether lengths for N=146 complexes with the gp3 DNA fragments. **(C & D)** Corresponding measurements for N=58 complexes after digestion of gp3 with proteinase K.

Fig. 3. Packaging of a 34.4 kbp DNA-gp3 construct longer than the native $\phi 29$ genome. The construct was produced by ligating together restriction fragments of λ and $\phi 29$ DNA. When translocation starts at the end of the DNA, as occurs with DNA lacking gp3, the tether shortens with a characteristic decreasing velocity profile (upper plot, gray line) due to the build-up of internal force resisting DNA confinement in the prohead. The DNA translocation stops after roughly one genome length has been packaged. With the DNA-gp3 construct the initial tether length is often shorter than full length, yet approximately the same total length of DNA is translocated during packaging (lower plots, black lines).

Fig. 4. Sucrose gradient sedimentation assays of the gp16 + DNA-gp3 reaction products

Fig. 5. Schematic model for the observed packaging of short DNA-gp3 tethers in the optical tweezers assay. **(A)** DNA-gp3 forms a loop mediated by gp3. **(B)** The gp16 domain of the motor binds the DNA-gp3 loop junction, resulting in a short DNA tether. **(C)** The loop is cleaved and the remaining DNA substrate is packaged.

Fig. 6. Schematic diagram of the fluid chamber with microsphere injection capillaries, described in the methods section.

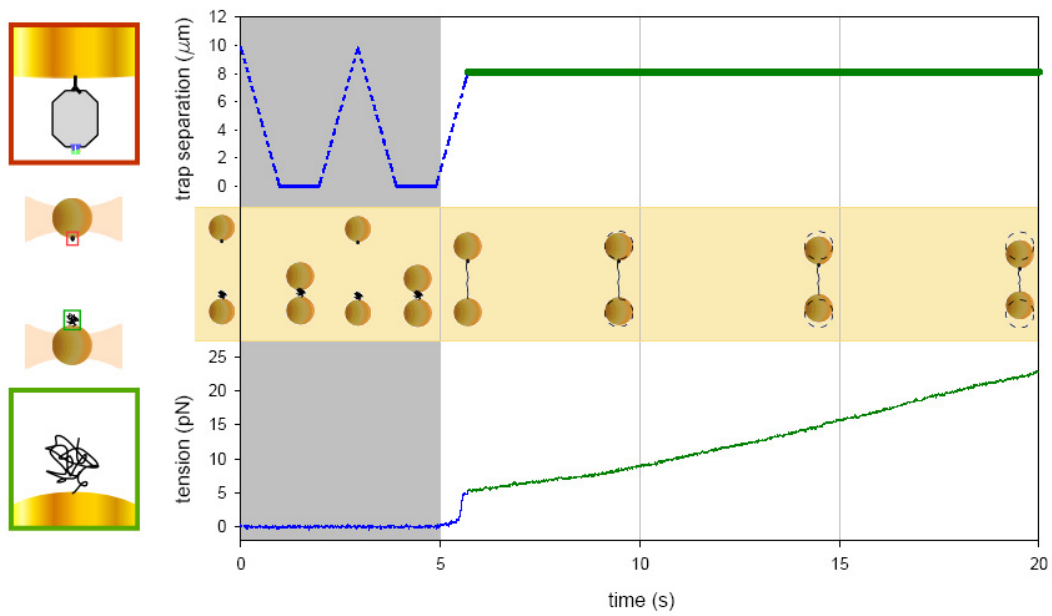


Fig. 1.

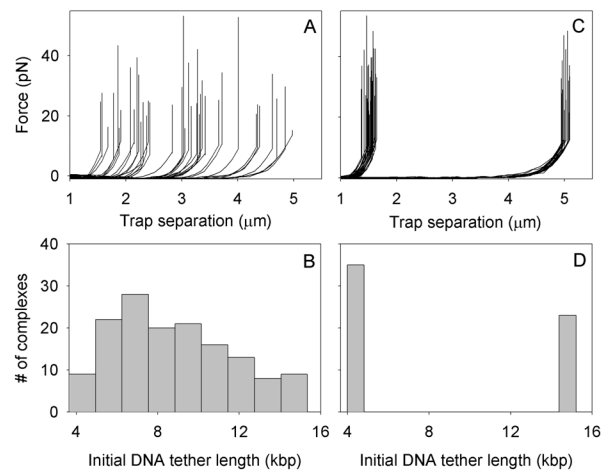


Fig. 2.

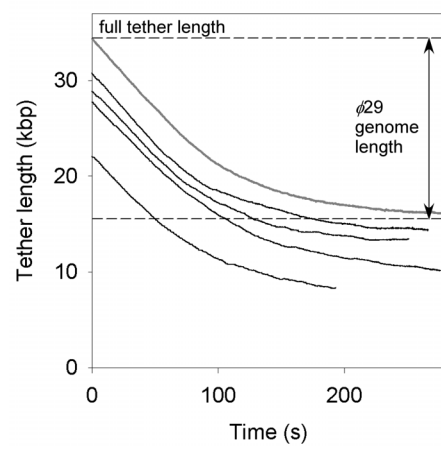


Fig. 3.

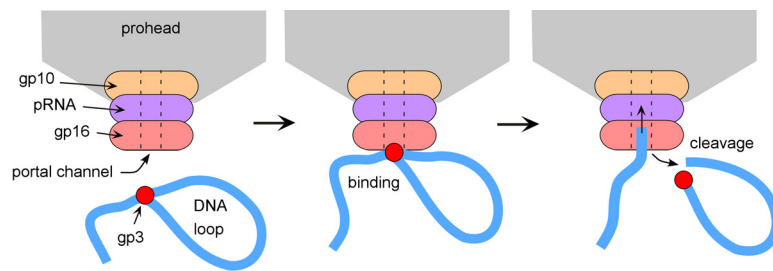


Fig. 5.

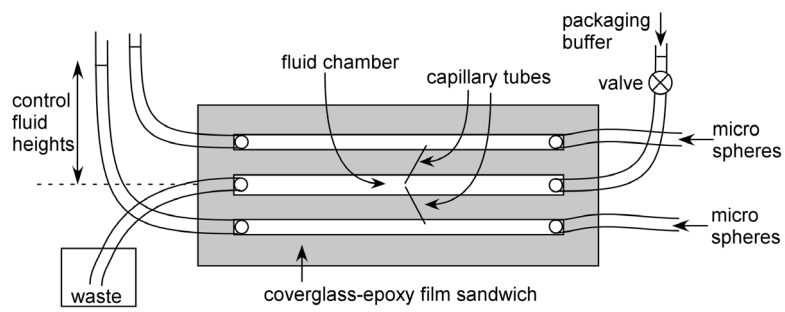


Fig. 6.